



Calcareous Nannofossil Biostratigraphy of Maastrichtian-Paleocene Oil Shales from Jordan

Abeer Al Zoubi¹ , Mohammad Alqudah^{2*} , Talal Al-Momani³ 

¹Department of Earth and Environmental Sciences, Faculty of Science, Yarmouk University, Irbid, Jordan.

^{2,3}Department of Earth and Environmental Sciences, Faculty of Science, Yarmouk University, Yarmouk, Jordan.

Article information

Received: 21- Jan -2024

Revised: 12- Mar -2024

Accepted: 13- Apr -2024

Available online: 01- Apr – 2025

Keywords:

Nannofossils

Biostratigraphy

Basin Architecture

Correspondence:

Name: Mohammad Alqudah

Email:

mohammad.alqudah@yu.edu.jo

ABSTRACT

Local biostratigraphic scheme based on calcareous nannofossil assemblages has been suggested in this work for upper Cretaceous and Paleocene oil shale successions. A total of 148 smear slides are studied from three oil shale boreholes throughout Jordan for their content of calcareous nannofossils. Six calcareous nannofossil biozones for Maastrichtian and nine zones for Paleocene are recognized from well OS-28. Cretaceous/Paleocene (K/P) and Paleocene/Eocene boundaries are detected either by calcareous nannofossil extinction or gamma ray. The K/P boundary appears to be missed. Although the short hiatus at K/P boundary is present, a distinctive gamma ray excursion remarked this boundary. Calcareous nannofossil assemblages were recovered gradually in the Danian, Complete biostratigraphic zones from Early Paleocene to Late Paleocene are recognized without any sedimentation break or hiatus in the central Jordan. Whereas uplift is proposed during Early to Late Paleocene to mark the hiatus in the northern and southern Jordan. Maastrichtian and Paleocene oil shales were deposited in the deep pelagic ramp, and the absence of allochthonous calcareous nannofossils provides strong evidence for that the sub-basins have not been exposed to winnowing and erosion process.

DOI: [10.33899/earth.2024.145606.1201](https://doi.org/10.33899/earth.2024.145606.1201), ©Authors, 2025, College of Science, University of Mosul.

This is an open access article under the CC BY 4.0 license (<http://creativecommons.org/licenses/by/4.0/>).

الطباقية الحياتية للمستحاثات النانوية من العصر الماسترختي - الباليوسيني لصخور السجيل الزيتية في الأردن

عبير الزعبي¹ ID، محمد القضاة^{2*} ID، طلال المومني³ ID

¹ قسم علوم الأرض والبيئة، كلية العلوم، جامعة العلوم، اربد، الأردن.

^{2,3} قسم علوم الأرض والبيئة، كلية العلوم، جامعة اليرموك، اليرموك، الأردن.

معلومات الارشفة	الملخص
تاريخ الاستلام: 21-يناير-2024	تم اقتراح مخططات طبقية حيوية محلية تعتمد على تجمعات الحفريات النانوية من أجل تصنيف الصخر الزيتي من العصر الطباشيري العلوي والباليوسيني. تمت دراسة ما مجموعه 148 شريحة من ثلاثة ابار نفطية من الأردن من أجل رسم الطبقات الحيوية الجيرية النانوية. تم التعرف على ست نطاقات حيوية أحفورية كلسية نانوية من عصر الماسترختيان وتوسع نطاقات للعصر الباليوسيني. من البئر OS-28، تم اكتشاف حدود العصر الطباشيري/العصر الباليوسيني إما عن طريق انقراض الحفريات الجيرية أو أشعة كاما. يبدو أن حدود K/P غير موجودة. على الرغم من أن الفجوة قصيرة عند حدود K/P، فقد لوحظ شذوذ مميز لأشعة كاما عند هذه الحدود. تم استخراج التجمعات الأحفورية الجيرية النانوية تدريجياً في عصر الدانيان، وقد تم التعرف على النطاقات الطباقية الحيوية الكاملة من العصر الباليوسيني المبكر إلى العصر الباليوسيني المتأخر دون أي انقطاع أو فجوة ترسيبية في وسط الأردن. في حين تم اقتراح ارتفاع البحر خلال العصر الباليوسيني المبكر والمتأخر ليشير إلى الفجوة التي لوحظت في شمالي وجنوبي الأردن. تم ترسيب الصخر الزيتي من عصر ماسترخت وباليوسين في المنحدر السطحي العميق. يشكل غياب الأحافير النانوية الجيرية المتجانسة دليلاً قوياً على أن الأحواض الفرعية لم تتعرض لعملية التعرية والتآكل.
تاريخ المراجعة: 12-مارس-2024	
تاريخ القبول: 13-ابريل-2024	
تاريخ النشر الإلكتروني: 01-ابريل-2025	
الكلمات المفتاحية: المستحاثات النانوية البيوستراتغرافية تركيب الحوض	
المراسلة: الاسم: محمد القضاة	
Email: mohammad.alqudah@yu.edu.jo	

DOI: [10.33899/earth.2024.145606.1201](https://doi.org/10.33899/earth.2024.145606.1201), ©Authors, 2025, College of Science, University of Mosul.
This is an open access article under the CC BY 4.0 license (<http://creativecommons.org/licenses/by/4.0/>).

Introduction

Enormous potential reserves of organic-rich marl deposits are reported in the Middle East in the Maastrichtian to Paleocene strata. Particularly in Jordan, these deposits are located in the north, center, and south with a various thicknesses reaching 200 m (Alqudah *et al.*, 2015). The micropaleontological studies already performed in this period are well constrained in Jordan. However, age framework concerning all the oil shale deposits in the south, center and north is still controversial.

Many biostratigraphical researches have been conducted in the north, central, and south of Jordan based on calcareous nannofossils, benthic and planktic foraminifera (e.g., Koch, 1968; Futyan, 1976; Hamam, 1977; Yassini, 1979; Basha, 1982; Naji, 1983; Nazzal and Mustafa, 1993; Smadi, 2003; Mihdawi and Mustafa, 2007; Alqudah *et al.*, 2014; Alqudah *et al.*, 2015; Farouk *et al.*, 2016; Beik *et al.*, 2017; Ahmad *et al.*, 2020). Organic-rich marl sediments were accumulated locally in this period in Jordan in anoxic sub-basins controlled tectonically by the shallow marine setting at the southern flank of Neo-Tethys (Powell and Mohd, 2011; Abed, 2013); for example, Yarmouk sub-basin at northern Azraq-Sirhan sub-basin and Lajjun sub-basin at central-, and Jafr sub-basin at southern Jordan (Fig. 1) (Abed *et al.*, 2005; Andrews, 1992). However, these sub-basins were formed due to a series of tectonic

compressional stresses at Jordan as an effect with the Syrian Arc (Powell, 1989; Abu-Jaber, 1989; Ziegler, 2001; Powell and Mohd, 2011).

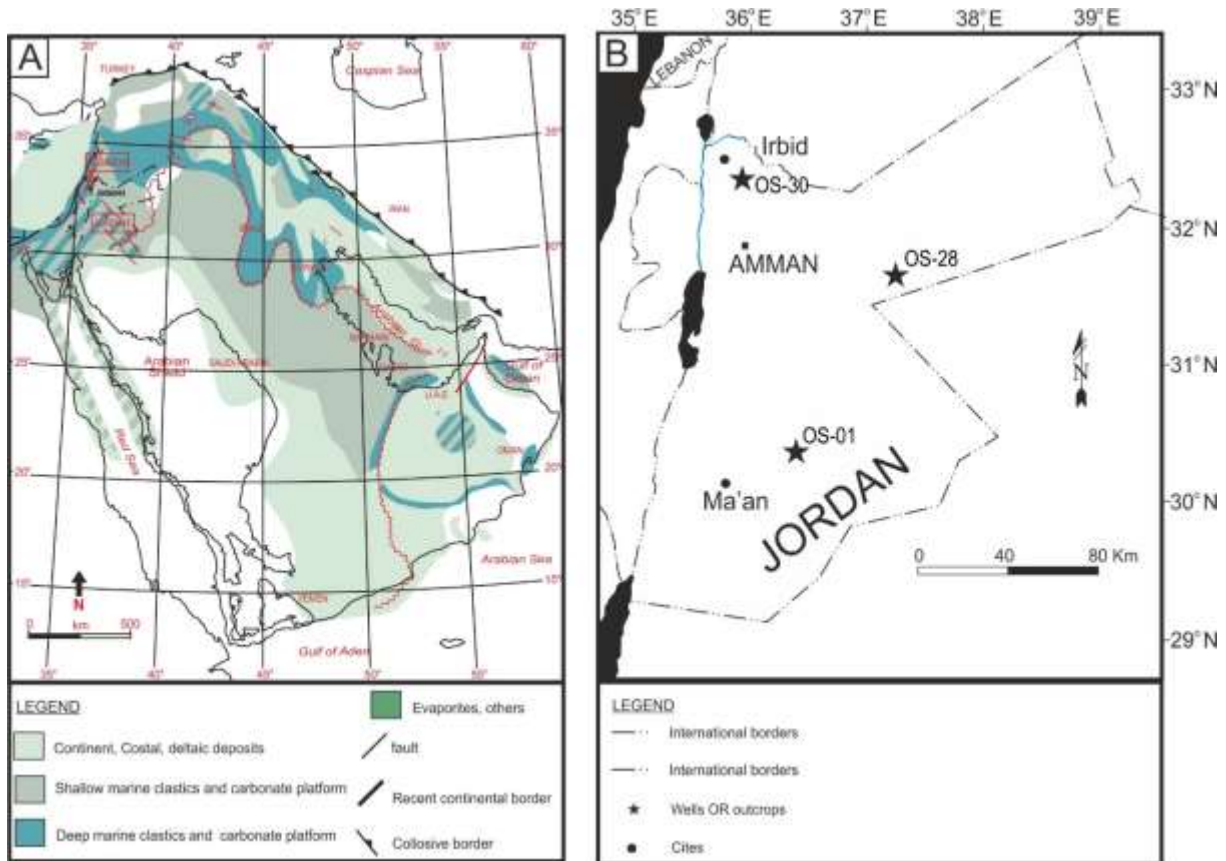


Fig. 1. (A) Paleofacies of the Maastrichtian period with deposition of the epicontinental sea in the northeast of Arabic Peninsula (after Ziegler, 2001). (B) Location map showing the current boreholes.

Calcareous nannofossils are suitable marker for age determination and correlations for Mesozoic and Cenozoic strata. Their geographic distribution is wide in between the open oceans to epicontinental seas (Mutterlose *et al.*, 2005). Mesozoic and Cenozoic biostratigraphic schemes are constructed based on the main stratigraphic events of the calcareous nannofossils (first and last occurrences of the specific taxa (e.g. Thierstein, 1976; Sissingh, 1977; Burnett, 1998 for Mesozoic, and Martini, 1970; Okada and Bukry, 1980 for Cenozoic). However, biostratigraphic schemes being in revised stage based on new finding which could attribute the old marker species (e.g., Bown, 2005; Fiorini *et al.*, 2012). Cretaceous-Paleocene boundary is a distinctive event. The calcareous nannofossils were recovered rapidly after this event and new genera were evolved from surviving species. Because of very diverse nature and time unknown affinities of the morphologic groups, thus all coccolithophore and associated non-coccolithophore nannolith are studied together to define the detailed scheme, e.g., *Prinsius* and *Toweius* from *Biscutum*, and *Discoaster* (Perch-Nielsen, 1985; Haq, 1998; Bown, 1998).

Aims of study

This study aims to provide a detailed biostratigraphic scheme of Maastrichtian and Paleocene strata and attempts to construct a framework that could have an impact on our understanding of oil shales deposition in the sub-basins of the late Cretaceous and early Paleocene times.

Geology

The onset of the locally organic-rich deposition was established in the Maastrichtian through a time extended from Maastrichtian to Paleocene, where oceanic settings and basins structure led to deposit deeper chalk-marl successions (Bender, 1975; Ziegler, 2001; Powell

and Mohd, 2011). Maastrichtian as well is characterized with a high sea stands as a result of global warming and submerge of southern Neo-Tethys to vast areas of Arabia (Abu-Jaber *et al.*, 1989; Alsharhan and Nairn, 1997). Accordingly, the chalk-marl successions intercalated with good quantity of organic-rich marls were pronounced in time from Maastrichtian to late Eocene and crossing through the boundary, which is noticeable by a depositional break in many sections in Jordan (e.g., Yassini, 1979; Smadi, 2003).

Lithology

Studied cores mainly consisting of organic-rich marl overlying chalky limestone layers are intercalated with chert bands at lower part (Ali Hussein *et al.*, 2014). Cretaceous-Paleocene boundary is recorded as bioturbated layers overlying the Cretaceous organic-rich marl. It is a yellow to pale brown and coarse-grained limestone with absence of organic matter. Calcareous nannofossils and other kinds of fossils are absent in this zone. Irregular surface characterizes the lower boundary, while layers are missed in this zone. The organic-rich marl reverts to appear throughout Paleocene with depletion in calcium carbonate content at Paleocene-Eocene boundary.

Methodology

Samples were taken from three cores in northern-, central-, and southern Jordan (Fig. 2). (OS-01 at south, 55 samples; OS-28 at center, 55 samples; OS-30 at north, 39 samples). Those cores were drilled by Jordan Oil Shale Company (Josco) during its oil shale project in Jordan. A total of 149 samples are prepared for calcareous nannofossil biostratigraphy. Calcareous nannofossils are examined by light microscopy with a magnification of 1250x. Biozones are given based on the first and last occurrence of index calcareous nannofossil species following Sissingh (1977), Burnett (1998) for Maastrichtian, and Martini (1970), Okada and Bukry (1980) for Paleocene. Roth (1973) is used to identify the preservation of calcareous nannofossils. Results are published in brief in Alqudah *et al.* (2015). Herein, the biostratigraphic comments are presented in detail with their implication for regional geology. Gamma ray data are gained from Jordan Oil Shale Company (Josco) for comparison purposes.

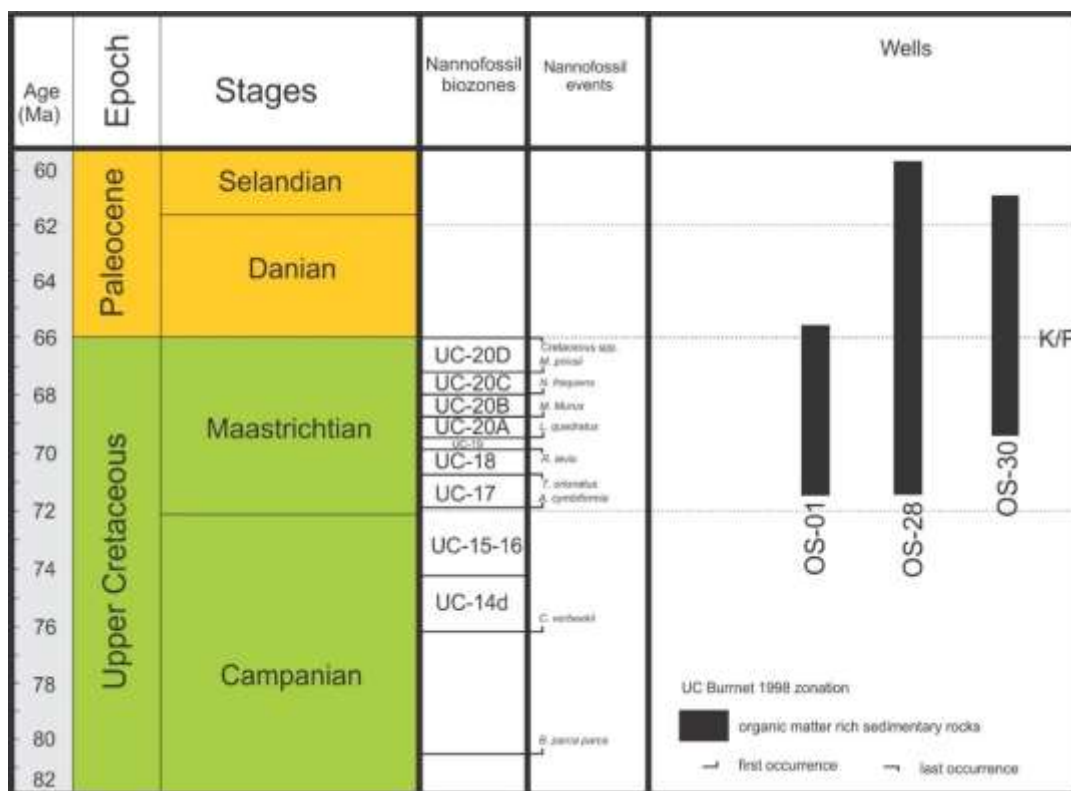


Fig. 2. Location and age of the three borehole cores (Alqudah *et al.*, 2015).

Results

Biostratigraphy

Maastrichtian

Broinsonia parca constricta is absent at the bottom of studied cores indicating that oil shales are not older than Early Maastrichtian age in the three cores. However, calcareous nannofossils are barren in the samples at 277-238 m, 184-153 m and 499-476 m of cores OS-01, OS-28 and OS-30 respectively. Distribution chart and occurrences of calcareous nannofossils are illustrated in Figure (3 A-C) and Plates (I and II). Samples 142-106 m of core OS-28 are assigned to the UC 17 zone based on the occurrence of *Tranolithus orionatus*. Calcareous nannofossils are rare in this biozone. The last occurrence of *Tranolithus orionatus* and the occurrence of *Reinhardtites levis* define the base of UC 18. Samples 237-219 m of core OS-01 are assigned to this biozone. While *Reinhardtites levis* is absent in core OS-28. Rare calcareous nannofossils have been recorded in all samples belonging to the UC 19 zone in intervals 214-206 m and 98-95 m and cores OS-01 and OS-28.

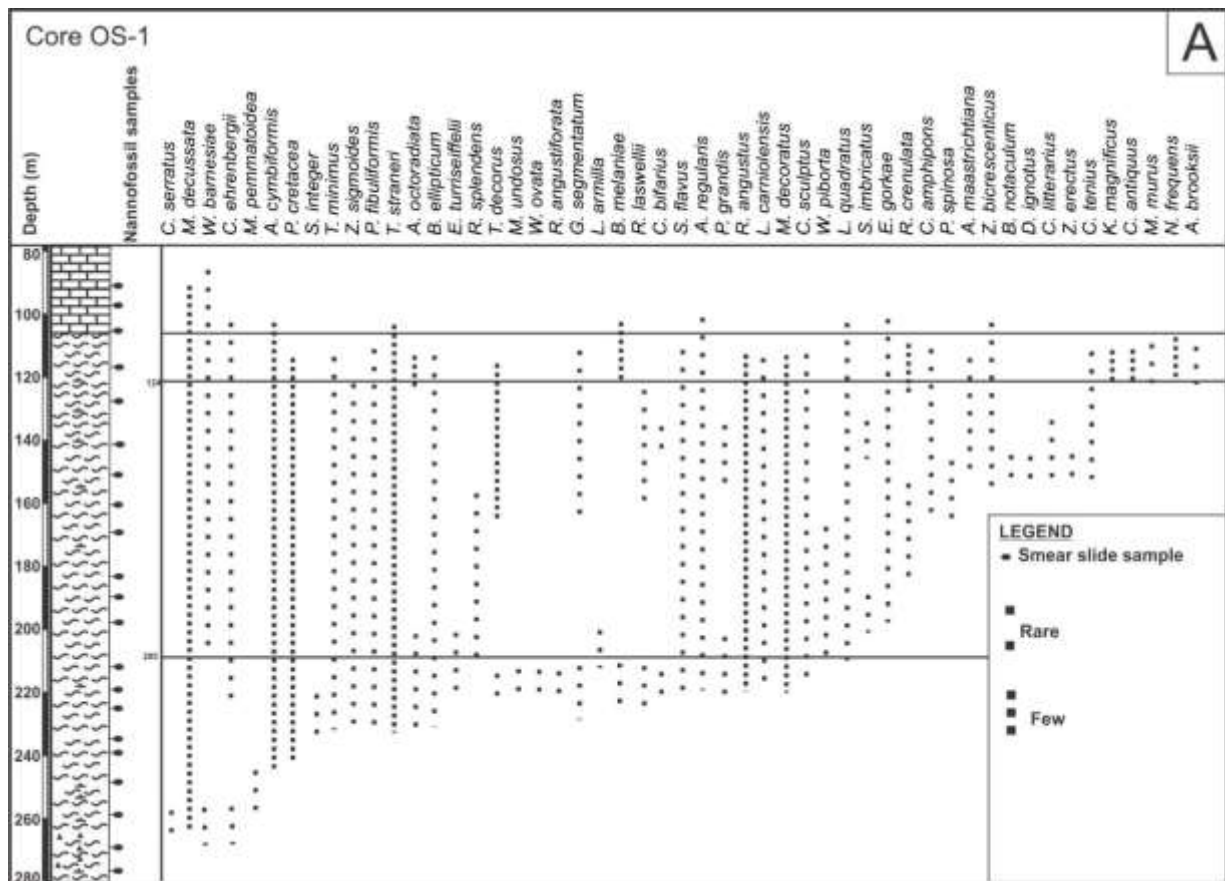


Fig. 3. A. Distribution chart and marker species picked from core OS-01.

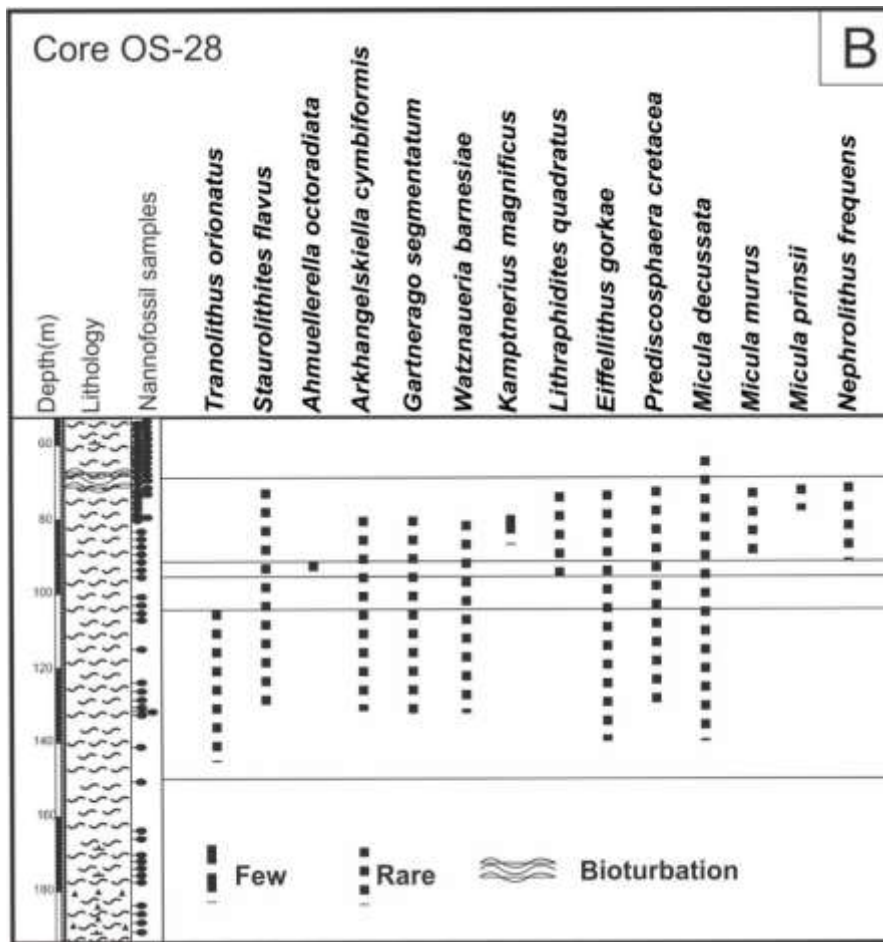


Fig. 3. B: Distribution chart and marker species picked from core OS-28.

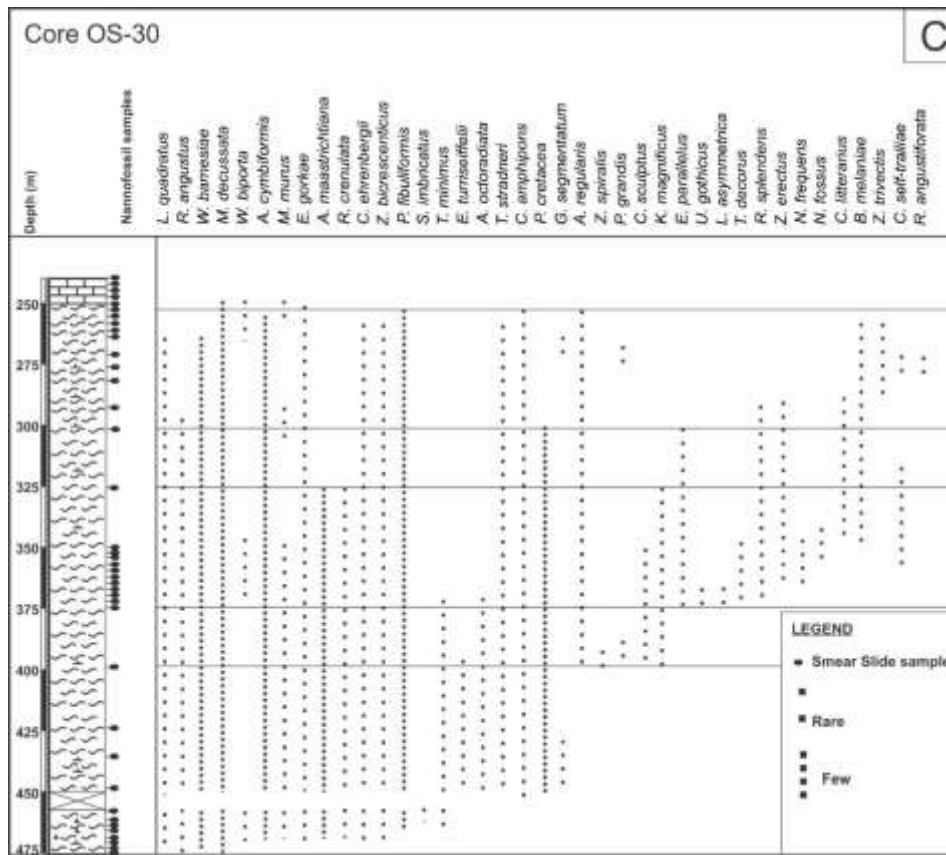


Fig. 3. C: Distribution chart and marker species picked from core OS-30.

Calcareous nannofossils had been flourished at late Maastrichtian as abundant, high diversity and well-preserved assemblages observed in the cores. The appearance of *Lithraphidites quadratus* (Plate 1) defines the base of the UC 20A. A thin interval of 473-472 m and 95-94 m represent this biozone in cores OS-28 and OS-30, while a thick interval 205-124 m of core OS-01 are recognized. Samples 124-114 m, 94-70 m and 473-249 m of cores OS-01, OS-28 and OS-30 respectively are given; the UC20B zone is based on the first occurrence of *Micula murus*. Abundant calcareous nannofossils have been observed in this biozone. The appearance of *Micula prinsii* defines the base of the UC20D biozone at sample no. 70 from the core OS-28. UC20D zone is missing in the cores OS-01 and OS-30.

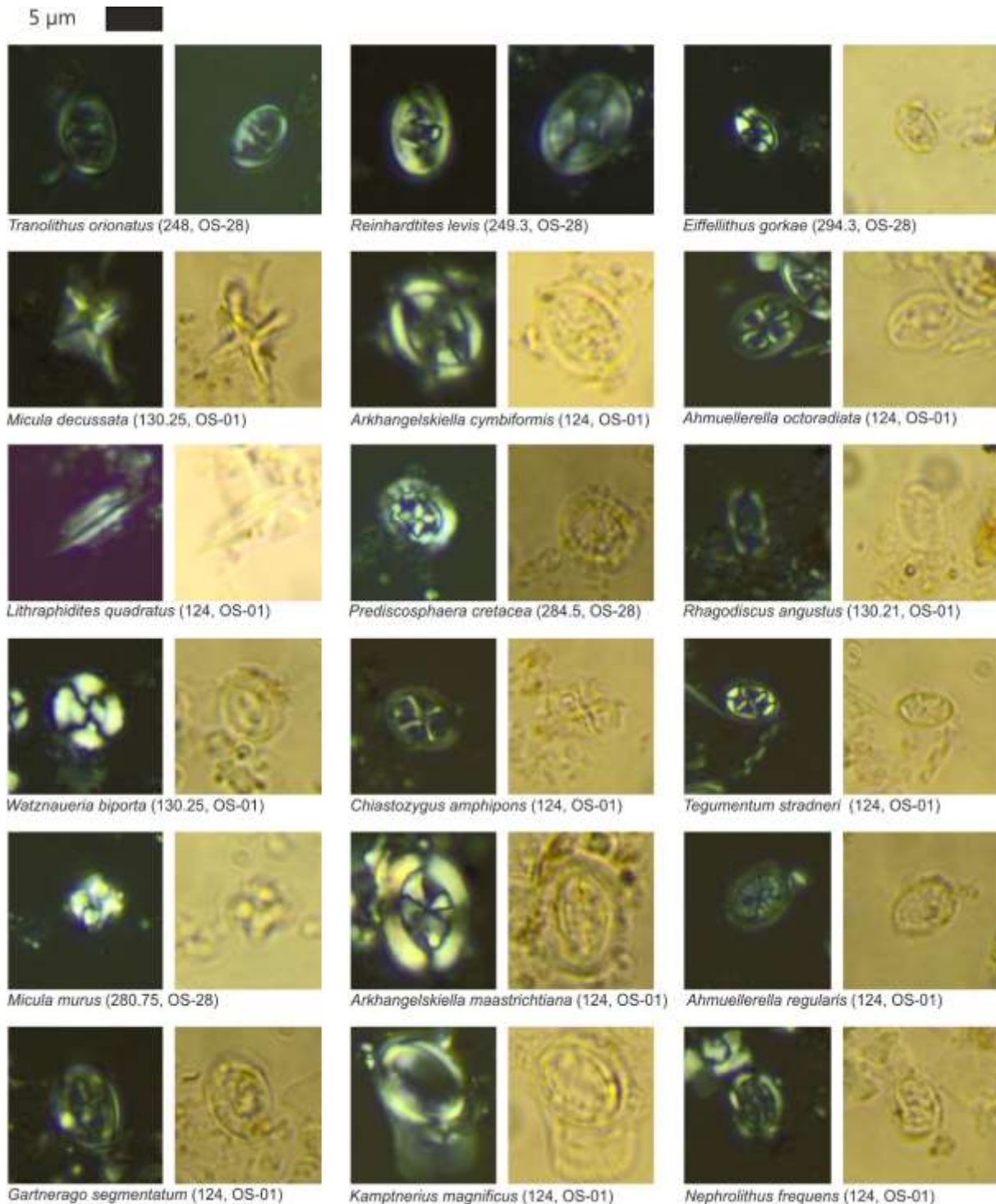


Plate 1. PPL and XPL micrographs of Maastrichtian calcareous nannofossil assemblages encountered in the samples.

Cretaceous-Paleocene boundary

Overlying the Maastrichtian organic-rich marl in the core OS-28, bioturbated layer intercalating with clay layer and very dark marl having high organic matter is obtained. A distinguish change in calcareous nannofossil abundance, where the majority of calcareous nannofossil species disappeared and only *Micula decussata* survived at samples 69 m. Cretaceous-Paleocene boundary is missing in the cores OS-01 and OS-30. Earliest Paleocene assemblages are found in the bioturbated layer.

Paleocene

Cyclagelosphaera reinhardtii, *Coccolithus cavus* and *Neocrepidolithus fossus* are recovered from the bioturbated zone just few centimeters above the Cretaceous Paleocene boundary at samples 69.3-69 m. The Cretaceous species *Micula decussata* and *Biscutum melaniae* are present in sample 69.1 m. Samples 114-109 m and 65-64 m are assigned to NP 2 based on the first occurrence of *Cruciplacolithus tenuis* (Plate 2). Species *Cruciplacolithus primus*, *Coccolithus pelagicus*, *Markalius inversus* and *Ericsonia robusta* have appeared within this biozone. The first occurrence of *Chiasmolithus danicus* defines the base of NP3 biozone. Samples 108-99 m and 64-63.25 m represent this biozones. A group of *Cruciplacolithus latipons*, *Neochiastozygus perfectus* and *Prinsius africanus* appeared in this biozone. While *Ellipsolithus macellus* is missing in the sample 63 m, the first occurrence of *Ellipsolithus distichus* was used to defines the base of NP 4, the first occurrence of *Chiasmolithus bidens* and *Sphenolithus primus* have detected in this biozone. Sample 59 m is assigned to NP 5 based on the first occurrence of *Fasciculithus tympaniformis*, the first occurrence of *Fasciculithus thomasi* has observed in this biozone. *Heliolithus kleinpellii* is missing in the sample 56 m, the first occurrence of *Toweius pertusus* defines the base of NP 6. The base of NP 7 was distinct in sample 50 m based on the first occurrence of *Discoaster mohleri* in this sample. *Toweius eminens* co-occurs with *Discoaster mohleri* in NP 7. Marker species like *Heliolithus riedelii* and *Discoaster nobilis* are missing in sample 48.7 m of core OS-28. The species *Zygodiscus adamas* are used for estimate the base of NP 8 in this sample. The first occurrence of *Sphenolithus anarrhopus* and *Neochiastozygus junctus* have found within this zone. The base of NP 9 was determined on samples 47.6 m 24.7 m of cores OS-28 and OS-30 based on the first occurrence of *Discoaster multiradiatus*, diverse calcareous nannofossils are observed in this biozone.

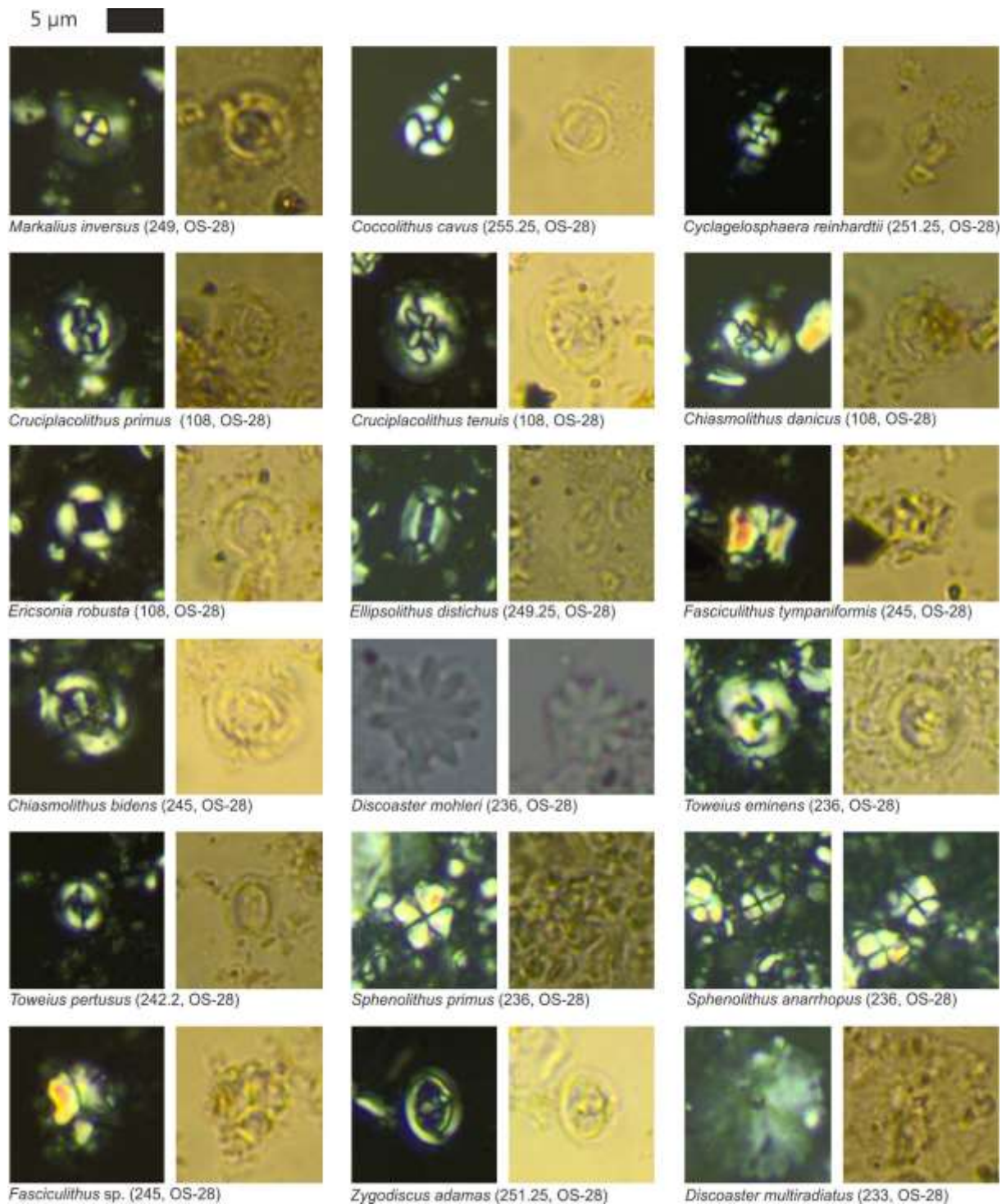


Plate 2. PPL and XPL micrograph of Paleocene calcareous nannofossil assemblages encountered in the samples.

Preservation abundance and reworking of calcareous nannofossils

Calcareous nannofossils in the biozones UC 17; UC 18 and UC 19 of Early Maastrichtian are remarkably poor preserved with rare abundance, missing of marker species due to preservation is proposed in those samples, this observation has swapped at the Late Maastrichtian assemblages in biozones UC 20A and B, where calcareous nannofossils are diverse, well preserved and abundant. Anyway, some horizons, e.g. 120-114 m of core OS-01, 78-69 m of core OS-28, 269-260 m and 256-249m of core OS-30, include poor preserved and rare calcareous nannofossils assemblages within Late Maastrichtian strata. Paleocene samples are remarked by well-preserved specimens. Diversity and abundance increased from Early to

Late Paleocene, maximum diversity and abundance of calcareous nannofossils are reported at NP 9. Allochthonous calcareous nannofossils are not observed in all samples.

Correlation

Correlations between three cores based on the calcareous nannofossil zones are illustrated in Figure (4). Calcareous nannofossils are barren at lower part of the three cores, Early-Late Maastrichtian zones are thick in the central- and southern Jordan, while it is absent in the north. Latest Maastrichtian of a thick UC20B zone has been detected in the north. Condense Danian (Early Paleocene) zones have been reported in the cores OS-01 and OS-28 in southern and central Jordan, while it is eroded in the north. Sedimentation break or hiatus is found in several horizons in different scales in the cores OS-01 and OS-30, while almost a complete biozone record is reported in the core OS-28 (Fig. 4). Latest Paleocene biozone (NP 9) is present in all cores.

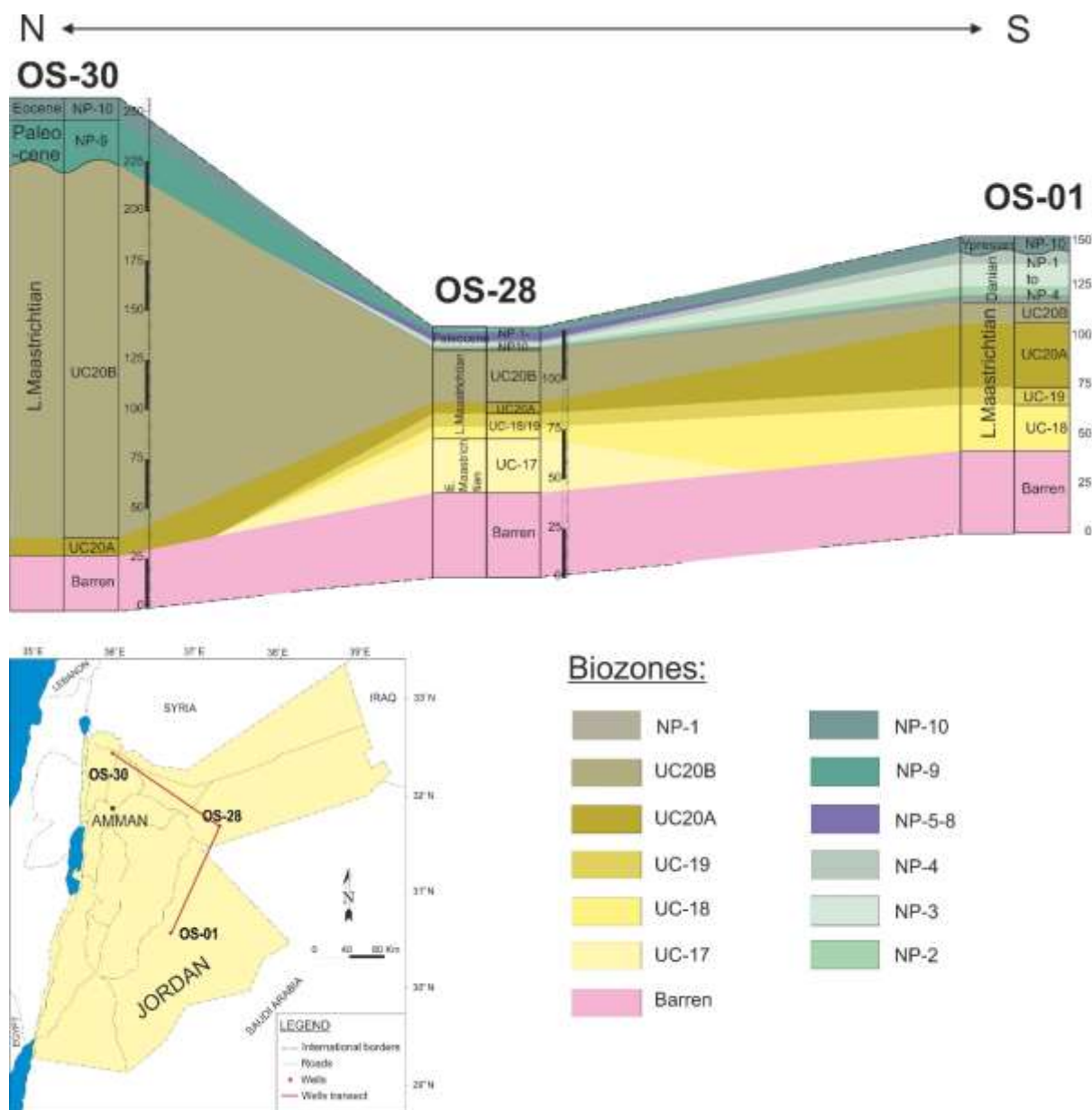


Fig. 4. Correlation between cores using calcareous nannofossils (Alqudah *et al.*, 2015).

Discussion

Gamma ray

Gamma ray data are drawn against the biostratigraphic data and illustrated in Figure (5). Many shifts have been recognized in the cores. Figure (6) provides one example from core OS-28. Two shifts of gamma ray at bottom of the core pointed to the boundary at the place of shifting. Lithology helps in understanding those shifts as the bottom of core includes layers of phosphates, which in turn could affect gamma ray readings. The major discordance in the interpretation here is that calcareous nannofossils are barren at bottom of the cores, which makes this correlation difficult to apply in term of time. A remarkable shift in gamma ray data is detected as well on the Cretaceous Paleocene boundary, the value reached approximately to 1000 CPS, then it dropped down to less than 200 CPS few centimeters above. This remarkable shift in gamma ray, as initial interpretation, could refer to an accumulation of clay minerals at the boundary or an abrupt change in facies due to rapid uplift. However, the Cretaceous-Paleogene Boundary was a bioturbated layer, which could reflect time of erosion and gap. Further investigation is needed at this stratigraphic level to confirm whether the iridium exists or not. Another shift in gamma ray is recorded at Paleocene-Eocene boundary. Alhejoj et al. (2020) reported unconformities in south of Jordan at both Cretaceous-Paleogene and Paleocene-Eocene boundaries indicating that sedimentological records were affected locally at the boundaries throughout Jordan.

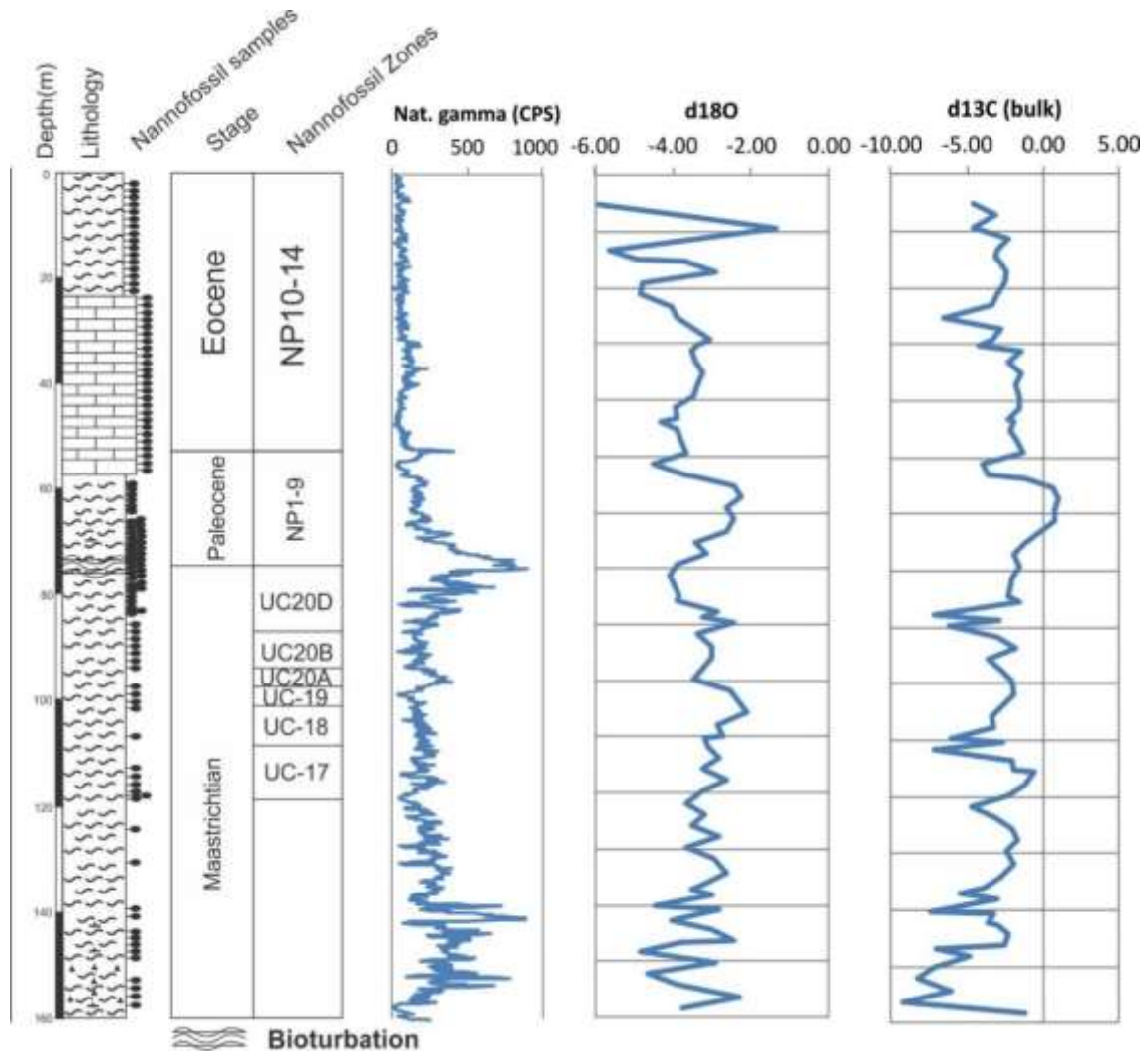


Fig. 5. Gamma ray covered Late Maastrichtian to Eocene, gamma ray gained from Jordan Oil Shale Company (Josco). Isotope data were taken from Beik et al. (2018).

Several major paleoclimatic and paleo-oceanographic fluctuations have been documented throughout the Maastrichtian-Paleocene interval using $\delta^{13}\text{C}$ and $\delta^{18}\text{O}$ records (Beik *et al.*, 2018; Farouk *et al.*, 2019; Farouk *et al.*, 2021). When focusing on $\delta^{13}\text{C}$ and $\delta^{18}\text{O}$ at the boundaries, a correlation can be made between them and the gamma ray record indicates that perturbation at the boundaries were established.

Biostratigraphy

The investigated Jordanian Maastrichtian biozones are local and rather correlated to Burnett (1998) zones than to Sissingh (1977) zones; where, for instance, *Nephrolithus frequens* is found earlier in its stratigraphic position than *Micula murus* (Fig. 6). The scarcities of some marker species at lower part of cores, especially UC 17, keep the biostratigraphic approach for correlation difficult to apply. Calcareous nannofossils are diverse in Late Maastrichtian, which enhances precise set up of the boundaries between biozones, break sedimentation or hiatus suggested by missing of uppermost strata in northern and southern Jordan, but still existing in central Jordan. Complete biostratigraphic zones from Early Maastrichtian to Late Paleocene have recorded without any sedimentation break or hiatus in central Jordan in core OS-28, except of missing in NP0 at the base of Paleocene, where bioturbation affected the preservation of calcareous nannofossils during earliest Paleocene time. However, these results could be a contrary to Farouk *et al.* (2014) results, who reported a hiatus in Jordanian sections. The result of core OS-30 in the north could fit with Smadi (2003), who suggested that Maastrichtian Paleocene boundary is a disconformity and Late Maastrichtian overlain by Late Paleocene. Naji (1983) suggested Late Maastrichtian overlain by Early Paleocene, but late Early Paleocene (NP 4 zone) overlain by latest Late Paleocene (NP 9 zone) with break sedimentation or hiatus have observed and biozones NP 5-8 are missing, this result is convenient with our finding in core OS-01 in the south.

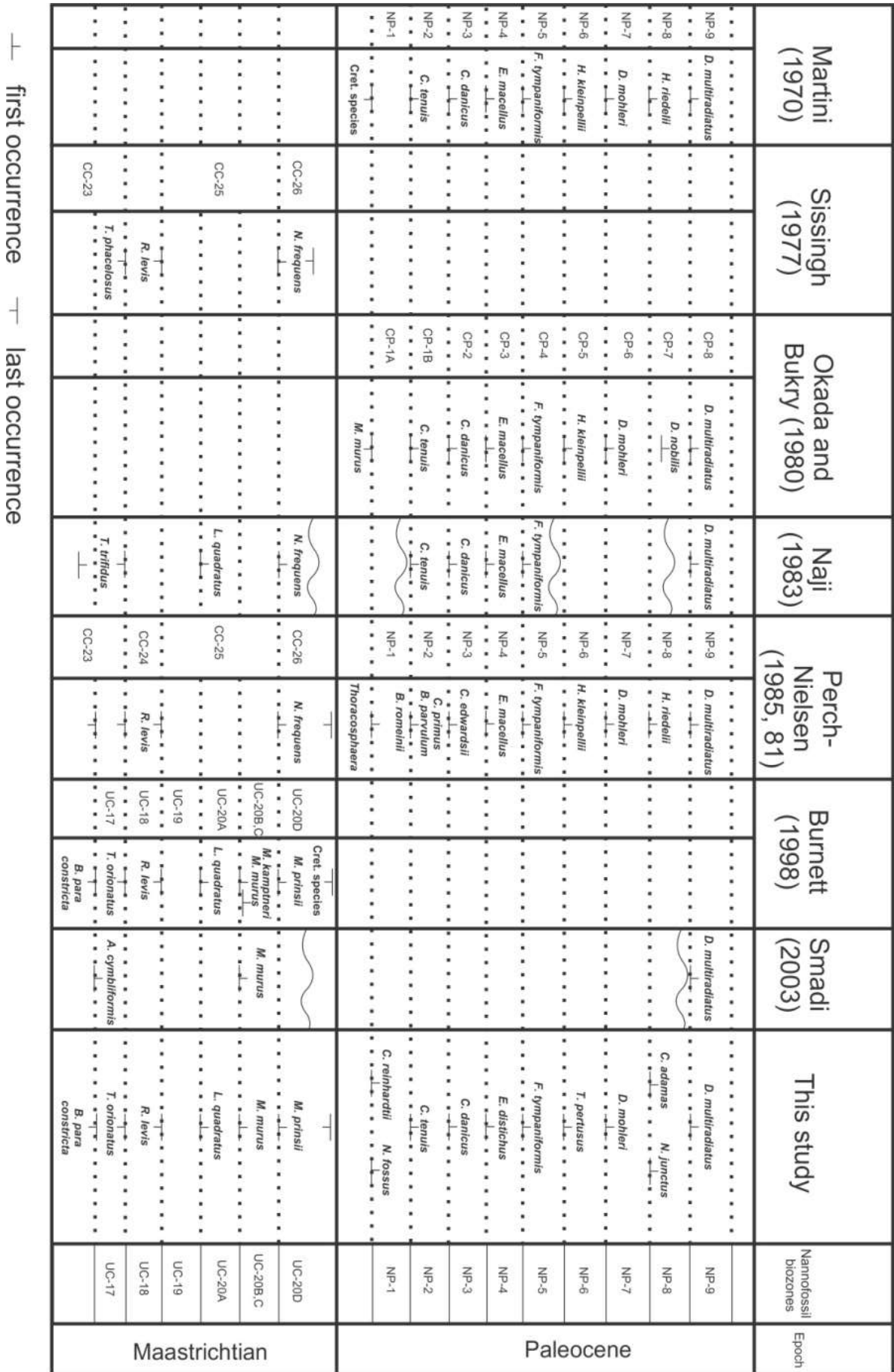


Fig. 6. Comparison between this study and the zonations of (Martini, 1970; Sissingh, 1977; Okada and Bukry, 1980; Naji, 1983; Perch-Nielsen, 1985; Burnett, 1998; Smadi, 2003).

Our Paleocene biozones are local too and correlated to Martini (1970) zones, marker species *Markalius inversus* is absent, anyway instead *Cyclagelosphaera reinhardtii* or *Neocrepidolithus fossus* are used. *Heliolithus riedelii* and *Heliolithus kleinpellii* are missing as well in the samples due to environmental condition unfavorable for these species, *Toweius pertusus* and *Zygodiscus adamas* are used as marker species.

Basin Construction of Late Cretaceous basins

Oil shales have been deposited in Maastrichtian-Paleocene in deep pelagic ramp with reported high sea level (Haq and Qahtani, 2005; Powell and Mohd, 2011). The basin never been exposed to winnowing and erosion process, and sub-basins located interiorly in the basin are characterized by a slug shallow water conditions at a level below storm wave-base, and oil shales deposited in these sub-basins. Swells have not any role to take in obstruct the movement of current came from east Neo-Tethys. These basins are characterized by ecologically stressed sea surface (Giraldo Gomez *et al.*, 2021).

First and last occurrences of calcareous nannofossil maker species are plotted in two wells from northern and southern Jordan against the one in the central Jordan (Fig. 7). Late Cretaceous basin was witnessed by two periods of sedimentation rates. The high sedimentation rate was recognized at the end of the Cretaceous simultaneously associated with the accumulation of organic matter in all Jordanian basins (north, center and south). These observations match with Hussein *et al.* (2023) finding, who investigated the sedimentation rate at north of Jordan Basins. Ahmad *et al.* (2014) and Giraldo Gomez *et al.* (2021) suggested influxes of upwelling deep water into the epicontinental sea during late Cretaceous and early Paleocene, which could enhance the primary production and therefore, increased the sedimentation rate.

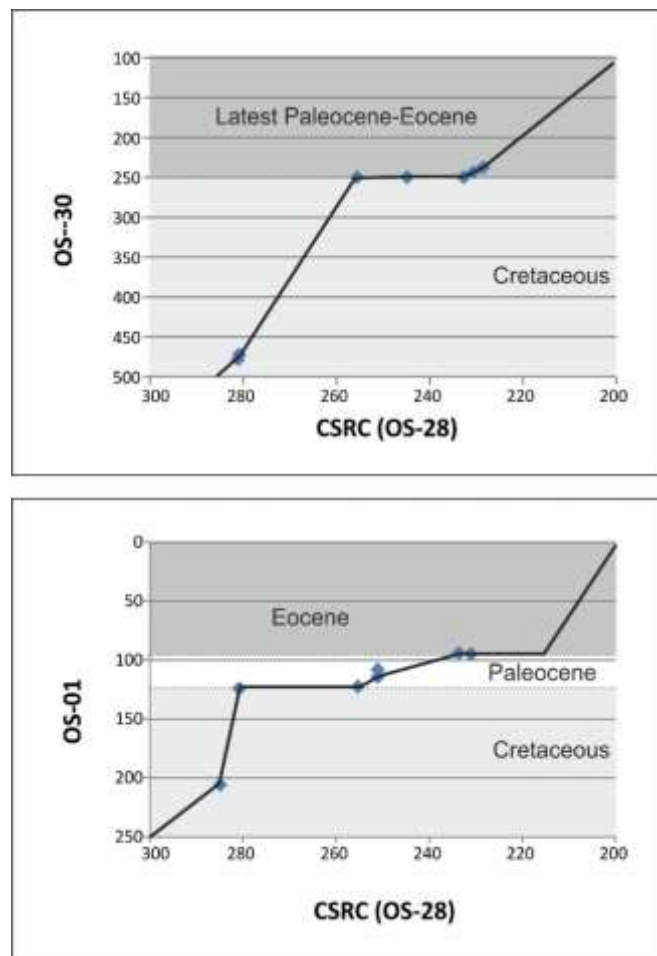


Fig. 7. Plots of OS-01 and OS-30 first and last occurrences of marker species versus occurrences in the composite section (OS-28).

Following the missing Cretaceous-Paleocene boundary and early Paleocene in north and south of Jordan as observed in the cores OS-01 and OS-30 due to Syrian Arc Fold System (Farouk *et al.*, 2016), Middle part of Paleocene is recognized as in the center and south of Jordan Basin. At least in time of Paleocene, hiatus appeared at south, while oil shales continued in accumulation in center and north of Jordan.

The unconformities are attributed to eustatic sea-level fluctuations and regional tectonics resulting from activation of the tectonic events (Farouk *et al.*, 2016). Existing of hiatus in the north or south of Jordan and observed shifting in oil shale facies through time indicated that uplift occurred due to Alpine Orogeny and closing of Neo-Tethys. This is proposed later in Paleocene and caused erosion of Early to Late Paleocene strata as shown by calcareous nannofossil zones. Uplift caused sedimentation break, which is a possible postulation to explain missing of calcareous nannofossil zones.

Conclusions

Results of this study can be concluded as follows:

1- Our local Maastrichtian and Paleocene biozones are correlated to Burnett (1998). Early Paleocene biozones can be correlated to Martini (1970) zones; however, few local marker species are used for Paleocene whenever the typical marker species are missed.

2- Complete biostratigraphic zones from Early Maastrichtian to Late Paleocene are found without any sedimentation break or hiatus in the central Jordan. Uplift was proposed during Early to Late Paleocene to explain the hiatus, which is observed in the northern and southern Jordan. Break sedimentation is a possible postulation to explain the missing of calcareous nannofossil zones. Distinctive Cretaceous Paleocene and Paleocene-Eocene boundary is detected either by calcareous nannofossils or/and gamma ray.

3- Maastrichtian and Paleocene oil shales were deposited in the deep pelagic ramp, and the absence of allochthonous calcareous nannofossils provides evidence that the sub-basins have not been exposed to winnowing and erosion process.

Conflict of Interest

The authors certify that they have no conflict of interest or affiliations with or involvement in any organization or entity with any financial interest, or non-financial interest in the subject matter or materials discussed in this manuscript.

References

- Abed, A., Arouri, K., and Boreham, C., 2005. Source Rock Potential of the Phosphorite–Bituminous Chalk–Marl Sequence in Jordan. *Marine and Petroleum Geology*, Vol. 22, pp. 413-425. DOI: [10.1016/j.marpetgeo.2004.12.004](https://doi.org/10.1016/j.marpetgeo.2004.12.004)
- Abed, A., 2013. The eastern Mediterranean phosphorite giants: An Interplay Between Tectonic and Upwelling. *Geo Arabia*, Vol. 18, No. 2, pp. 67-94. <https://doi.org/10.2113/geoarabia180267>
- Abu-Jaber, N., Kimberly, M., and Cavaroc, V., 1989. Mesozoic-Paleogene Basin Development Within the Eastern Mediterranean Borderland. *Journal of Petroleum Geology*, v. 12, n. 4, pp. 419-436. <https://doi.org/10.1111/j.1747-5457.1989.tb00241.x>
- Ahmad, F., Farouk, S., Abd El-Moghny, M.W., 2014. A Regional Stratigraphic Correlation for the Upper Campanian Phosphorites and Associated Rocks in Egypt and Jordan. *Proceedings of the Geologists' Association*, Vol. 125 (4), pp. 419-431. <https://doi.org/10.1016/j.pgeola.2014.06.002>

- Ahmad, F., Faris, M., Farouk, S., 2020. Calcareous Nannofossil Biostratigraphy and Carbon Isotopes from the Strato Type Section of the Middle Eocene Wadi Shallala Formation, Northwestern Jordan. *Jordan Journal of Earth and Environmental Sciences*, Vol. 11 (2), pp. 103-112.
- Alhejoj, I., Farouk, S., Bazeen, Y.S., Ahmad, F., 2020. Depositional sequences and sea-level changes of the upper Maastrichtian-middle Eocene Succession in Central Jordan: Evidence from Foraminiferal Biostratigraphy and Paleoenvironments. *Journal of African Earth Sciences*, Vol. 161, pp. 103663. <https://doi.org/10.1016/j.jafrearsci.2019.103663>
- Ali Hussein, M., Alqudah, M., Van den Boorn, S., Podlaha, O.G., Mutterlose, J., 2014. Ichnofabrics of Eocene Oil Shales from Central Jordan and Their Use in Paleoenvironmental Reconstructions. *Geo Arabia*, Vol. 19, No. 1, pp. 143-158. <https://doi.org/10.2113/geoarabia190185>
- Alqudah, M., Ali Hussein, M., van den Boorn, Giraldo, V., S., Kolonic, S., Podlaha, O.G., Mutterlose, J., 2014. Eocene Oil Shales from Jordan- Paleoenvironmental Implications from Reworked Microfossils. *Marine and Petroleum Geology*, Vol. 52, pp. 93-106. <http://dx.doi.org/10.1016/j.marpetgeo.2014.02.001>
- Alqudah, M., Ali Hussein, M., Vom Boemer, S., Podlaha, O.G., Mutterlose, J., 2015. Biostratigraphy and Depositional Setting of Maastrichtian - Eocene Oil Shales from Jordan. *Marine and Petroleum Geology*, Vol. 60, pp. 87-104. <http://dx.doi.org/10.1016/j.marpetgeo.2014.07.025>
- Alsharhan, A. and A. Nairn., 1997. *Sedimentary Basins and Petroleum Geology of the Middle East*. Elsevier Science B.V., Amsterdam, 843 P.
- Andrews, I., 1992. Cretaceous and Paleogene Lithostratigraphy in the Subsurface of Jordan: NRA. Bulletin, No. 5, 60 P.
- Basha, S., 1982. Stratigraphy, Paleogeography and Oil Possibilities of the Azraq Sirhan Turayf Basin (Jordan-Saudi Arabia). *Dirasat*, Vol. 9, pp. 85-106.
- Beik, I., Giraldo Gemez, V., Podlaha, Olaf, Mutterlose, J., 2017. Microfacies and depositional Environment of the Late Cretaceous to Early Paleocene Oil Shales from Jordan. *Arabian Journal of Geosciences*. Vol. 10, pp.346. <https://doi.org/10.1007/s12517-017-3118-6>
- Beik, I., Giraldo Gemez, V., Podlaha, Olaf, Mutterlose, J., 2018. The $\delta^{13}\text{C}$ Record of Maastrichtian-Paleocene Oil Shales from Jordan – Stratigraphic and Environmental Implications for an Epicontinental Setting. *Journal of African Earth Sciences*. Vol. 143, pp.134-144. <https://doi.org/10.1016/j.jafrearsci.2018.03.022>
- Bender, F., 1975. *Geology of the Arabian Peninsula-Jordan*. United States Geological Survey Professional Paper 560-I, Washington, 36 P. <https://doi.org/10.3133/pp560I>
- Bown, P., 1998. *Calcareous Nannofossil Biostratigraphy*. British Micropaleontology Society Publications Series. Kluwer Academic Publishers, London, 315 P. <http://dx.doi.org/10.1007/978-94-011-4902-0>
- Bown, P., 2005. Paleogene Calcareous Nannofossils from the Kilwa and Lindi Areas of Coastal Tanzania (Tanzania Drilling Project 2003-4). *Journal of Nannoplankton Research*, Vol. 27, No. 1, pp. 21-95. <https://doi.org/10.58998/jnr2031>
- Burnett, J., 1998. Upper Cretaceous. In P. Bown (Ed.), *Calcareous Nannofossils Biostratigraphy*. Chapman and Hall, London, pp. 132-199. <http://dx.doi.org/10.1007/978-94-011-4902-0>
- Farouk, S., Marzouk, A.M., Ahmad F., 2014. The Cretaceous Paleocene Boundary in Jordan. *Journal of Asian Earth Sciences* Vol. 94, pp. 113-125. <https://doi.org/10.1016/j.jseaes.2014.08.015>

- Farouk, S., Ahmad F., Powell J., Marzouk, A.M., 2016. Integrated Microfossil Biostratigraphy, Facies Distribution, and Depositional Sequences of the Upper Turonian to Campanian Succession in Northeast Egypt and Jordan. *Facies* Vol. 62 (8). <https://doi.org/10.1007/s10347-016-0461-0>
- Farouk, S., Jain, S., Faris, M., Elamri, Z., Ahmad, F., 2019. Campanian Carbon Isotope Calibrated Paleofertility Estimates from Northwestern Tunisia: Inferences from Calcareous Nannofossils. *Marine Micropaleontology* Vol. 148, pp. 78-102. <https://doi.org/10.1016/j.marmicro.2019.03.009>
- Farouk, S., Faris, M., Bazeen, Y.Z., Elamri, Z., Ahmad, F., 2021. Upper Campanian-Lower Maastrichtian integrated carbon isotope Stratigraphy and Calcareous Microplankton Biostratigraphy of North-Central Tunisia. *Marine Micropaleontology* Vol. 166, pp. 102003 <https://doi.org/10.1016/j.marmicro.2021.102003>
- Fioroni, C., G. Villa, D. Persico, S. Wise and L. Pea., 2012. Revised Middle Eocene-Upper Oligocene Calcareous Nannofossil Biozonation for the Southern Ocean. *Revue de Micropaléontologie*, v. 55, No. 2, pp. 53-70. <https://doi.org/10.1016/j.revmic.2012.03.001>
- Futyan, A., 1976. Late Mesozoic and Early Cianozoic Benthic Foraminifera from Jordan. *Paleontology*, Vol. 19, No. 3, pp.517-537.
- Giraldo-Gómez, V.M., Mutterlose, J., Beik, I., Podlaha, O.G., Kolonic, S., 2021. Oil Shales from the K-Pg boundary Interval of Jordan – Climate controlled Archives of Surface and Bottom Water Conditions in a Shelf Setting. *Marine and Petroleum Geology*, Vol. 123, pp. 104724. <https://doi.org/10.1016/j.marpetgeo.2020.104724>
- Hamam, K., 1977. Foraminifera from the Maastrichtian phosphate-bearing strata of El-hasa, Jordan. *Journal of foraminiferal research*, Vol. 7, No. 1, pp. 34-43.
- Haq, B., 1998. Calcareous nannoplankton. In B. Haq and A. Boersma (Eds.), *Introduction to Marine Micropaleontology*, Elsevier Science (Singapore) Pte Ltd., Singapore, pp. 79-108.
- Haq, B. and A. Al-Qahtani, 2005. Phanerozoic Cycles of Sea-Level Change on the Arabian Platform. *Geo Arabia*, 10, No. 2, pp. 127-160. <https://doi.org/10.2113/geoarabia1002127>
- Hussein A., Al-Tarawneh, O., Alqudah, M., 2023. Calcareous Nannofossils Biostratigraphy of Late Cretaceous–Paleocene Successions from Northern Jordan and their Implications for Basin Analysis. *Geosciences* 13, pp. 351. <https://doi.org/10.3390/geosciences13110351>
- Koch, W., 1968. Zur Micropaläntologie und Biostratigraphy der Oberkreide und des Alttertiärs von Jordanien. *Geologisches Jahrbuch*, heft 85, pp. 627-668.
- Martini, E., 1970. Standard Paleogene calcareous nannoplankton zonation. *Nature*, Vol. 226, pp. 560-561. <https://doi.org/10.1038/226560a0>
- Mihdawi, H. and H. Mustafa, 2007. Petrography and Geochemistry of the Upper Cretaceous-Lower Tertiary oil Shale, NW-Jordan. *Abhath Al-Yarmouk*, Pure Science and Engineering Series, Vol. 16, No. 2, pp. 293-318.
- Mutterlose, J., Bornemann, A., Herrle, J.O., 2005. Mesozoic Calcareous Nannofossils-State of the Art. *Palaontologische Zeitschrift* 79, 113-133. <https://doi.org/10.1007/BF03021757>
- Naji, F., 1983. Kalkiges Nannoplankton aus der Oberkreide und dem Alttertiär Nord Jordaniens (Mittel-Santon bis Eozän). *Geologisches Jahrbuch*, Reihe B: Regionale Geologie Ausland, Vol. 55, pp. 3-185.
- Nazzal, J. and H. Mustafa, 1993. Ammonites from the Upper Cretaceous of North Jordan. *Abhath Al-Yarmouk*, Pure Science and Engineering Series, Vol. 2, No. 2, pp. 87-120.

- Okada, H. and D. Bukry, 1980. Supplementary Modification and Introduction of Code Numbers to the Low Latitude Coccolith Bio Stratigraphic Zonation (Bukry, 1973, 1975). *Marine Micropaleontology*, Vol. 5, pp. 321-325. [http://dx.doi.org/10.1016/0377-8398\(80\)90016-X](http://dx.doi.org/10.1016/0377-8398(80)90016-X)
- Perch-Nielsen, K., 1985. Cenozoic Calcareous Nannofossils. In H.M. Bolli, J.B. Saunders and K. Perch-Nielsen (Eds.), *Plankton Stratigraphy*. Cambridge University Press, Cambridge, pp. 427-554.
- Powell, J., 1989. Stratigraphy and Sedimentation of the Phanerozoic Rocks in Central and South Jordan. Part B: Kurnub, Ajlun and Belqa Group. *Geological Mapping Division Bulletin* 11, Natural Resources Authority, Amman, 130 P.
- Powell, J. and B. Moh'd., 2011. Evolution of Cretaceous to Eocene Alluvial and Carbonate Platform Sequences in Central and South Jordan. *Geo Arabia*, Vol. 16, No. 4, pp. 29-82. <https://doi.org/10.2113/geoarabia160429>
- Roth, P., 1973. Calcareous Nannofossils-Leg 17, Deep Sea Drilling Project. In E.L. Winterer and J.I. Ewing (Eds.), *Initial Reports of the Deep-Sea Drilling Project*, Vol. 17, pp. 695-795.
- Smadi, A., 2003. Cretaceous-Paleogene Biostratigraphy Successions in Jordan. *Dirasat, pure science*, Vol. 30, No. 2, pp. 262-282.
- Sissingh W., 1977. Biostratigraphy of Cretaceous Calcareous Nannoplankton. *Geologie en Mijnbouw*, Vol. 57, pp. 433-440.
- Thierstein, H., 1976. Mesozoic Calcareous Nannoplankton Biostratigraphy of Marine Sediments. *Marine Micropaleontology*, Vol. 1, pp. 325-362. [https://doi.org/10.1016/0377-8398\(76\)90015-3](https://doi.org/10.1016/0377-8398(76)90015-3)
- Yassini, I., 1979. Maastrichtian-Lower Eocene Biostratigraphy and the Planktonic Foraminiferal Biozonation in Jordan. *Revista Espanola de Micropaleontologia*, v. 11, pp. 5-57.
- Ziegler, M., 2001. Late Permian to Holocene paleofacies evolution of the Arabian Plate and its hydrocarbon occurrences. *GeoArabia*, Vol. 6, No. 3, pp. 445-504. <https://doi.org/10.2113/geoarabia0603445>